The International Journal of Advanced Manufacturing Technology (2021) 116:1169–1177
https://doi.org/10.1007/s00170-021-07478-5

ORIGINAL ARTICLE

A flexible and economical method for electromagnetic flanging of tubes with field shapers

Qi Xiong [1,2] · Zhe Li [1,2] · Jianhua Tang [3] · Hang Zhou [1,2] · Meng Yang [4] · Xianqi Song [1,2]

Received: 10 January 2021 / Accepted: 11 June 2021 / Published online: 29 June 2021

Abstract

Recent years have witnessed the rapid development of electromagnetic flanging of tubes, which uses coils to generate electromagnetic forces to achieve the deformation with high speed but without contact. However, the electromagnetic force decays dramatically with the increase of distance, resulting in strict requirements of geometrical matching between the coils and the tubes. Usually, new coils should be fabricated for tubes with new sizes, which is inconvenient and uneconomical. Therefore, a more flexible and economical method is proposed in this paper, which introduces a solenoid field shaper into the existing electromagnetic flanging system. By adjusting the structure and the position of the field shaper, the distribution of electromagnetic forces can be reshaped to form tubes with various sizes, without changing the coil, whose cost is much higher than a field shaper. The principle of this method is introduced in detail. Then, an electromagnetic-structure coupled finite element simulation model is established to calculate the forming process. The results show that when forming an A6063-T83 aluminum alloy tube with an inner diameter of 110mm, the discharge voltage can be tuned down from 5.3kV, without field shaper, to 4.6kV, with field shaper. That means the energy consumption of the system can be saved by 25%, and the manufacturing process of the field shaper is simpler than that of the forming coil. What's more, when forming tubes with different sizes, the new method shows higher effectiveness, greater flexibility, and lower cost than the traditional way.

Keywords Electromagnetic flanging · Field shaper · Tube · Electromagnetic force · Flexibility

1 Introduction

The flanging of metal tubes is a common processing technology in the industry, and the parts have usually been used in manufacturing fields such as automobiles, aerospace, and instruments. When flanging metal tubes with traditional technology, the process is very cumbersome and requires multiple working procedures. However, electromagnetic flanging is a more effective method to achieve the flanging of aluminum alloy tubes. Electromagnetic flanging is a technology that uses non-contact pulsed electromagnetic force to drive metal tubes to deform. It has a series of advantages such as faster forming speed, higher forming limit, and less spring back [1]. Moreover, some specific workpieces can only be completed by electromagnetic flanging, so many scholars have been carrying out unremitting research on electromagnetic flanging [2]. Yu et al. used the magnetic pulse forming process to flange the AA 3003-O aluminum alloy tube to improve the flanging formability limit. The results showed that there are critical discharge energy values for the flanging dies with varied slope angle [3]. Xiong et al. proposed the electromagnetic flanging of the tube which is based on the attractive electromagnetic force generated by the improved double coils [4]. However, the new coils should be fabricated for tubes with new sizes, in all the above methods, which is neither convenient nor economical.

The reason for the above problem is that, in the process of flanging the tube, the electromagnetic force decays rapidly as

✉ Qi Xiong
pandaqi0218@gmail.com

1 College of Electrical Engineering & New Energy, China Three Gorges University, Yichang 443002, China

2 Hubei Provincial Engineering Technology Research Center for Power Transmission Line, China Three Gorges University, Yichang 443002, China

3 School of Civil Engineering, Lanzhou University of Technology, Lanzhou 730050, China

4 Suixi Power Supply Company, State Grid Anhui Electric Power Co.Ltd., Huaibei 235100, China

the distance increases, resulting in strict requirements of geometrical matching between the coils and the tubes. For tubes with larger inner diameters, larger-shaped coils need to be selected. On the one hand, new coils should be fabricated for tubes with new sizes. For different tube sizes, different coils need to be replaced, which is inconvenient. On the other hand, the winding process of the coil is very complicated, and frequent replacement of the coil will increase the cost.

In order to solve these problems, a flanging forming method of the tube with a field shaper is proposed in this article. A solenoid field shaper is introduced into the existing electromagnetic flanging system. By adjusting the structure and the position of the field shaper, the distribution of electromagnetic forces can be reshaped to form tubes of various sizes, without changing the coil, whose cost is much higher than that of the field shaper. The field shaper is a kind of commonly used low-cost auxiliary accessories, which can change the distribution of magnetic fields and strengthen the magnetic field in the local area by adjusting its structure, and is widely used in the processing technology of the workpiece. Gharghabi et al. analyzed the influence of tube thickness and geometry of field shaper on the whole discharge system [5]. Rajak et al. studied different types of field shapers and analyzed the working efficiency of these types of field shapers. Their research methods are also applicable to the design and research of bulging field shapers [6]. Zhang et al. proposed a novel field shaper with a slow-varying central hole, and the experimental results show that the field shaper can effectively improve the size of the welding region [7]. To verify this method, an electromagnetic-structure coupling finite element simulation model is established. A series of simulations have been carried out with this model and their results are shown below.

2 Principle and design

2.1 Traditional electromagnetic flanging

The traditional electromagnetic flanging system of the tube mainly includes a charging system, a capacitor power supply, an air switch, a coil, a tube, and a fly-wheel circuit. Its principle is shown in Fig. 1a. First, the charging system charges the capacitor banks. After the charging is completed, the stored energy is released to the coil through the air switch, thereby generating an instantaneous pulse current. The current generates a strong pulsed magnetic field, which in turn excites an induced eddy current in the tube. The interaction between the induced eddy current and the magnetic field generates a strong repulsive force, which drives the tube to deform, and can be expressed as [8]

$$\boldsymbol{F} = \boldsymbol{J}_e \times \boldsymbol{B} \tag{1}$$

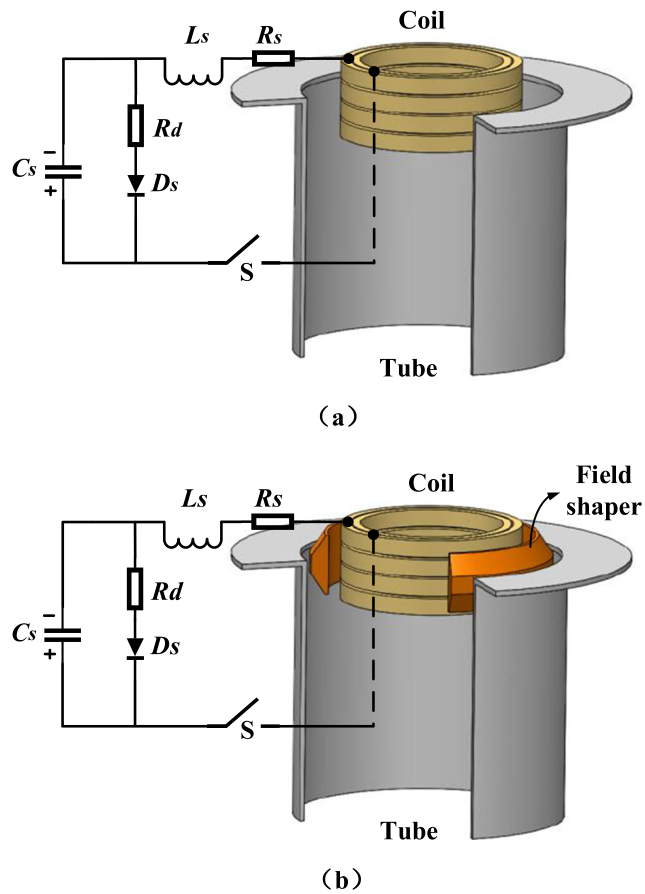

Fig. 1 Schematic diagram of electromagnetic flanging system: (**a**) without field shaper; (**b**) with field shaper

where $\boldsymbol{B}$ and $\boldsymbol{J}_e$ are magnetic flux density and eddy currents density of tube. Electromagnetic force can be decomposed into axial and radial components in the analysis of an electromagnetic flanging process [9], which are called radial Lorentz force and axial Lorentz force, and they are determined by [10]:

$$\boldsymbol{F}_r = \boldsymbol{J}_e \times \boldsymbol{B}_z \tag{2}$$

$$\boldsymbol{F}_z = -\boldsymbol{J}_e \times \boldsymbol{B}_r \tag{3}$$

where $\boldsymbol{B}_z$ and $\boldsymbol{B}_r$ are the radial component and the axial component of the magnetic flux density respectively.

2.2 Electromagnetic flanging with a field shaper

The field shaper is a commonly used auxiliary accessory to strengthen the magnetic field in a specific area during the electromagnetic forming. It mainly uses the skin effect and the unique structure to cooperate with each other to transmit the induced eddy current of the coil, so as to change the position and shape of the magnetic field generated by the forming coil. As a matter of fact, the structure of the field shaper is a rotating conductor, which is generally composed of high-conductivity metal materials, such as copper and aluminum.

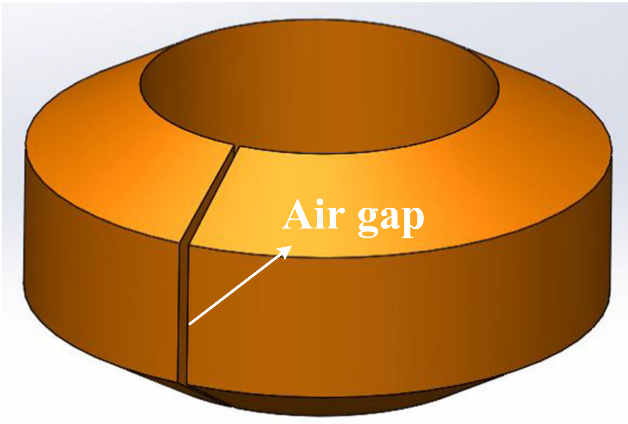

Fig. 2 Structure diagram of solenoid field shaper

As shown in Fig. 2, this article uses a solenoid field shaper, made of the same material as the molded coil. The solenoid field shaper has two surfaces in the structure. The height of the inner surface is much larger than that of the outer surface, and there is an air gap in its longitudinal direction. According to the literature, the influence of the air gap can be ignored, so the three-dimensional model is simplified to a two-dimensional axisymmetric model in this paper [11].

When introduced into the tube flanging forming system, the field shaper is located between the coil and the tube, as shown in Fig. 1b. Due to the skin effect and Lenz's law, this induced eddy current flows to the outer surface of the field shaper from the axial slot [12]. Therefore, the current direction is the same as which in the coil. Accordingly, the energy of the forming coil is transferred from the forming coil to the workpiece, equivalent to shorten the distance. The skin depth is determined by

$$\Delta = \sqrt{\frac{1}{\pi\sigma\mu f}} \tag{4}$$

where μ is the permeability and σ and f are the conductivity and frequency of the current. The design principle of field shaper in electromagnetic flanging is similar to it. The induction vortex of the forming coil in the metal workpiece is mainly concentrated on the surface area of the workpiece. Therefore, the design idea of a field shaper comes from this.

The simplified diagram of the existing electromagnetic flanging process is shown in Fig. 3a. If a larger tube (Tube2) is to be formed, a larger forming coil (Coil2) needs to be replaced as shown in Fig. 3b, which is undoubtedly more complicated. Based on this, this article adds a field shaper to the system as shown in Fig. 3c. Without changing the coil, the magnetic field configuration generated by the forming coil is changed by the field shaper, so that the magnetic field lines are concentrated on the area to be flanged, and the flanging effect of the tube is optimized.

3 Simulations

The main purpose of this paper is to analyze and compare the flanging effects of tubes with different sizes. Thereby, three tubes with different inner diameters are selected for numerical simulation. Numerical simulation is one of the indispensable methods in the study of the electromagnetic forming process. In this paper, based on COMSOL, the electromagnetic-structure coupled FEM simulation model of the tube is established, as shown in Fig. 4, to simulate the plastic deformation process of aluminum alloy tubes in a time-varying electromagnetic field.

3.1 Circuits

The discharge circuit is the "engine" of electromagnetic flanging technology, which provides the transient change of discharge current for the forming coil. At present, the most

Fig. 3 Schematic diagram of electromagnetic flanging: (**a**) initial coil; (**b**) coil change; (**c**) coil unchange

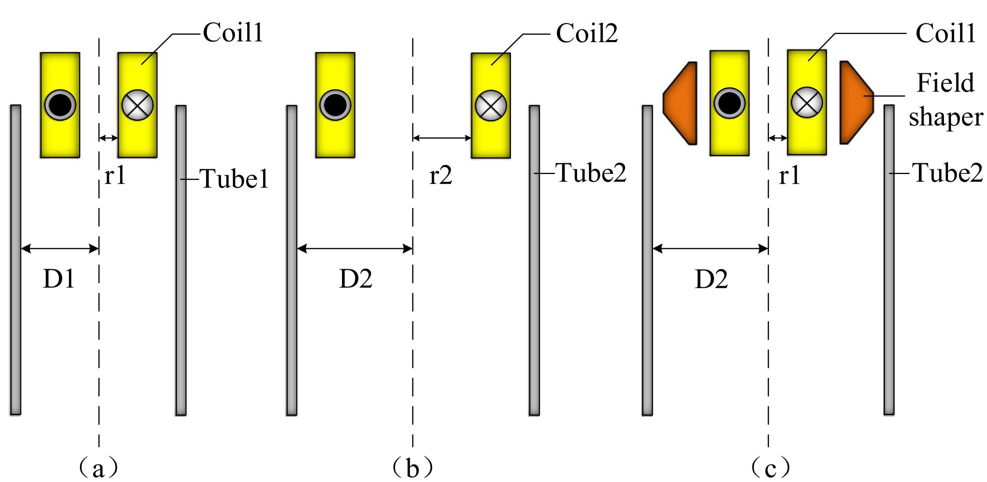

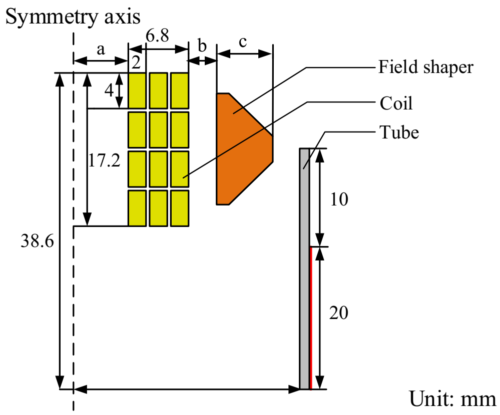

Fig. 4 The geometry of numerical simulation

common RLC discharge circuit is based on a capacitor. The equivalent circuit is shown in Fig. 5.

The discharge circuit equation with freewheeling loop is as follows:

$$U_c = (R_l + R_c) I_{coil} + L_l \frac{d I_{coil}}{d t} + \left(\frac{d L_c I_{coil}}{d t} + \frac{d M I_w}{d t} \right) \tag{5}$$

$$I_{coil} + I_c - I_d = 0 \tag{6}$$

$$U_c = U_0 + \frac{1}{C} \int_0^t I_c \, d t \tag{7}$$

The conditions that the current in the freewheeling loop meets:

$$\begin{cases} I_d = 0 & (U_c > 0) \\ I_d = \dfrac{U_c}{R_d} & (U_c < 0) \end{cases} \tag{8}$$

where I_{coil} is the discharge current loaded by the forming coil, I_w is the induced current in the tube, U_0 is the initial voltage of the capacitor, and M is the mutual inductance between the forming coil and the tube.

It is worth mentioning that M is closely related to the coupling coefficient in the electromagnetic flanging system. In electromagnetic flanging, since the tube is in a transient continuous change process, the mutual inductance of the system also follows its transient change, that is, M is a continuously changing quantity.

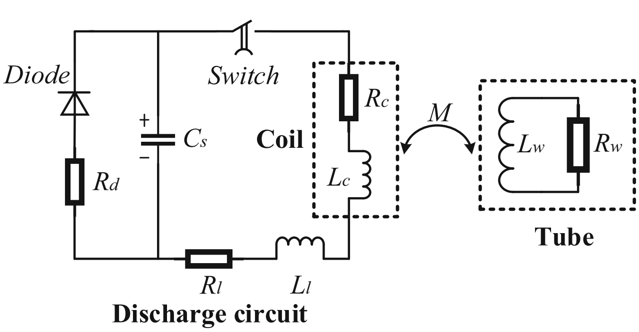

Fig. 5 Equivalent schematic diagram without field shaper

Based on the above circuit, a field shaper is introduced in this paper, which is located between the forming coil and the tube as shown in Fig. 6. For this reason, the physical parameters in the electromagnetic flanging system will change. The relevant parameters are consistent except the discharge voltage, and the detailed parameters are shown in Table 1.

It can be concluded that the coupling equivalent inductance has changed after the introduction of the field shaper. In the original electromagnetic flanging system, the coupling equivalent inductance between the tube and the forming coil is M, which is changed to $M_{c\text{-}w}$+ $M_{c\text{-}f}$. In addition, the coupling equivalent inductance between the tube and the field shaper is $M_{f\text{-}w}$. From the point of view of the circuit, it is not difficult to see that the function of the field shaper is to transfer the induced current generated by the forming coil. After introducing the field shaper into the electromagnetic flanging system, the discharge circuit equation is as follows:

$$U_c = (R_l + R_c) I_{coil} + L_l \frac{d I_{coil}}{d t} + \left(\frac{d L_c I_{coil}}{d t} + \frac{d M_{c\text{-}f} I_f}{d t} + \frac{d M_{c\text{-}w} I_w}{d t} \right) \tag{9}$$

where I_{coil} is the discharge current loaded by the forming coil and I_w is the induced current in the tube.

3.2 Material

The electromagnetic force at each point of the tube calculated by Eq. (1) is used as the load in the structure field to cause the tube to flange, and the deformation at each point of the tube is solved by the following equilibrium equation [13]:

$$\nabla \cdot \sigma + F = \rho \frac{\partial^2 u}{\partial t^2} \tag{10}$$

where ρ and u are the density and the displacement vector and σ and F are the stress tensor and the electromagnetic force

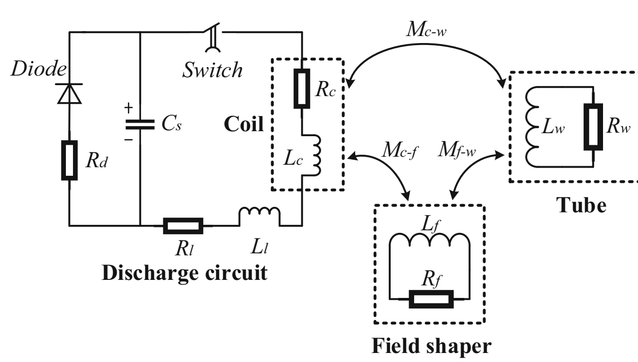

Fig. 6 Equivalent schematic diagram with field shaper

Table 1 Circuit parameters

Discharge parameters	Symbol	Value
Capacitance	C	160uF
Line resistance	R_{ex}	8mΩ
Line inductance	L_{ex}	10uF
Crowbar resistance	R_d	10mΩ

Table 2 The parameters of tube

Parameters	Value
The length of tube	30mm
The thickness of tube	1mm
The material of tube	6063-T83
Density	2.7g/cm^3
Electrical conductivity	3.03×10^{7}S/m
Relative permittivity	1
Relative permeability	1
Young's modulus	6.9×10^{10}Pa
Poisson's ratio	0.33
Initial yield tensile strength	2.3×10^{8}Pa

density.

In the calculation of the structural field, the choice of the constitutive equation of material is very important. The constitutive equation mainly describes the relationship between stress and strain during material deformation and reflects the characteristics of material deformation behavior. For different deformation behaviors, the selection of the constitutive equation directly affects the accuracy of numerical simulation results. On the basis of the engineering material characteristics database (https://www.makeitfrom.com/material-properties/6063-T83-Aluminum), this paper did a tensile experiment on A6063-T83 aluminum alloy, and obtained the real parameters of the tube.The thickness and length of the tubes are 1mm and 30mm, and the material parameters are shown in Table 2.

With the continuous deepening of materials science research, various constitutive equations that can accurately describe the deformation behavior of materials have been developed. In this paper, only electromagnetic flanging at room temperature is considered, and temperature change is not considered. Therefore, the Cowper-Symonds constitutive model considering only high strain is adopted. The constitutive equation is as follows [14, 15]:

$$\sigma = \sigma_y \left[1 + \left(\frac{\dot{\varepsilon}}{C} \right)^m \right] \tag{11}$$

where σ_y and ε are the yield stress and the plastic strain rate and C and m are constant.

4 Results and discussions

4.1 The effectiveness

The flanging angle in Fig. 7 is defined as θ to measure the flanging effect of the tube, which can be calculated as follows:

$$\begin{cases} \theta = \arctan \dfrac{|Dr|}{10\text{-}|Dz|} & |Dz| < 6.2 \\ \theta = 90^\circ & |Dz| = 6.2 \\ \theta > 90^\circ & |Dz| > 6.2 \end{cases} \tag{12}$$

where D_r and D_z are the radial displacement and axial displacement of point A, and point B is the constraint point of the tube. When θ is 90°($|D_z|$=6.2mm), the tube reaches the optimal flanging effect.

Figure 8 shows the flanging effect of tubes under the same forming coil. The inner diameters of the tubes are 100mm and 110mm respectively in Fig. 8a and b. With the same discharge voltage (3kV), it can be seen that the tube in Fig. 8a has a significant flanging degree, and the tube in Fig. 8b is not deformed. In reality, θ is reduced from 13 to 0° in Fig. 8a and b. The electromagnetic force decays rapidly with the increase of distance, resulting in strict requirements of geometrical matching between the coils and the tubes. Comparing the two models, it can be concluded that θ decreases rapidly with the increase of the inner diameter of the tube.

After introducing a field shaper into the model, it can be seen that the tube has reached the desired degree of flanging (θ_3=90°) as shown in Fig. 8c. The length of the inner surface and outer surface of the field shaper is 12.6mm and 5.2mm, respectively, and the thickness is 4mm. At this time, the

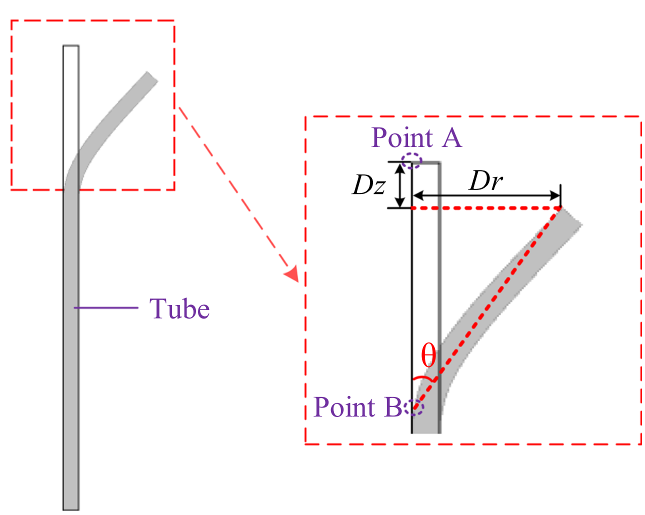

Fig. 7 Calculation of flanging angle (defined as θ)

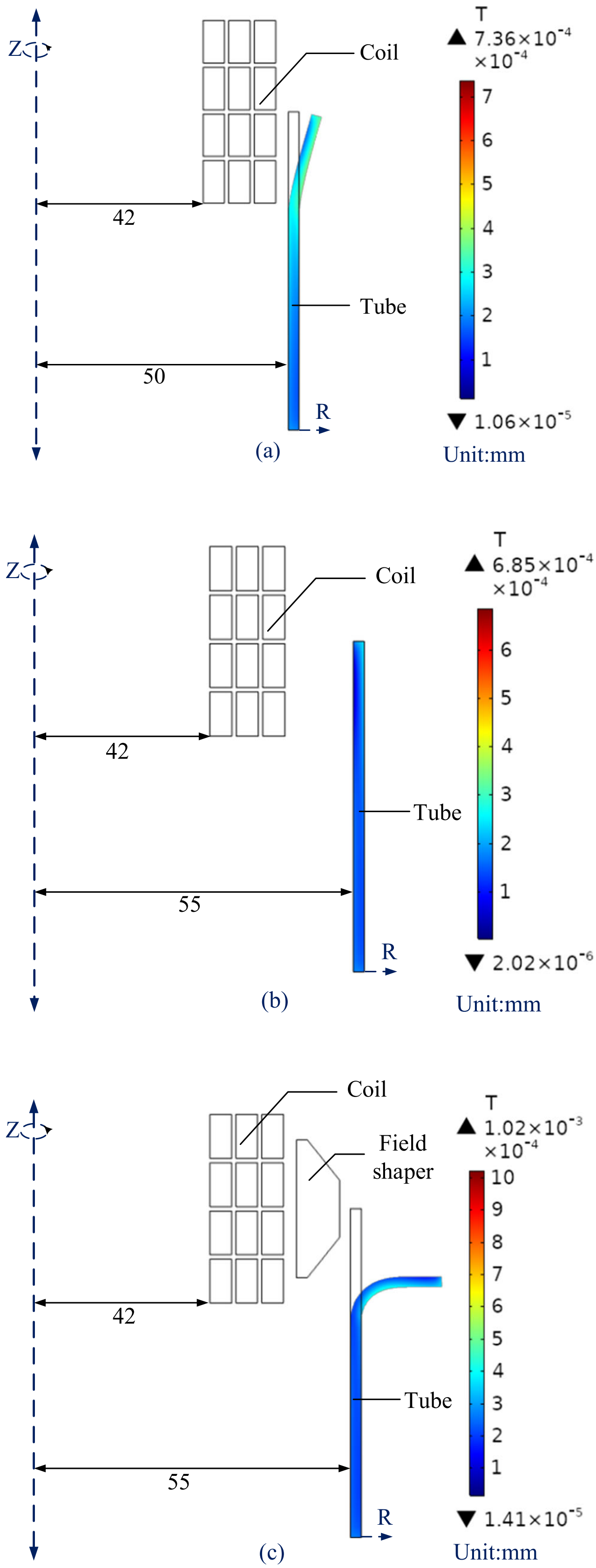

Fig. 8 Comparison diagram of tube flanging: (**a**) and (**b**) without field shaper; (**c**) with field shaper

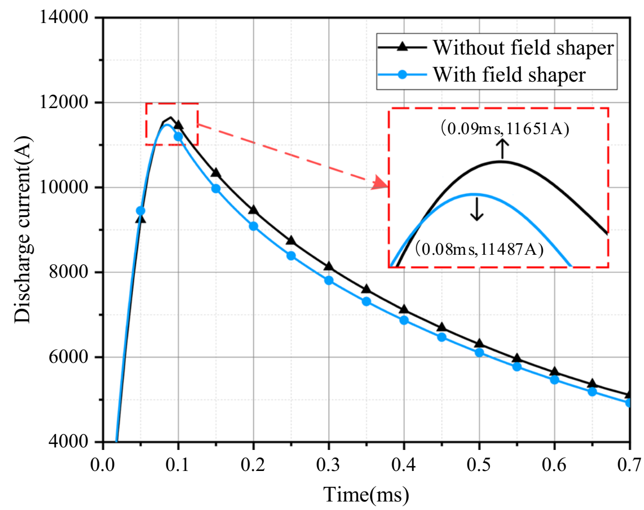

Fig. 9 Waveforms of discharge currents

discharge voltage increases to 4.6kV. This means that the field shaper can effectively improve the flanging effect of tubes.

With the same discharge energy (1.69kJ), the current waveform is shown in Fig. 9. From the diagram, it can be seen that after the field shaper is added to the entire system, the time at which the discharge current reaches the peak value is advanced by 0.01ms. The main reason is that after introducing the field shaper, $\boldsymbol{M}$ in Eq. (5) becomes the superposition of $\boldsymbol{M}_{c\text{-}w}$ and $\boldsymbol{M}_{c\text{-}f}$ in Eq. (9), and the equivalent inductance of the formed coil increases, resulting in the decrease in the pulse width of the discharge current.

Figure 10 shows the distribution of the Lorentz force vector during the electromagnetic flanging process. It can be seen that at different moments, the degree of tube rotation is greater relative to the system without field shaper. This is mainly due to the field shaper that strengthens the magnetic field in the flanged area of the tube, thus making the electromagnetic force more concentrated.

In this paper, the radial displacements of tubes under different models are calculated as shown in Fig. 11. It can be concluded that under the same discharge energy, the radial displacement of the tube in the system with field shaper is larger. The radial maximum values of point A are 8.433mm and 2.833mm respectively. By comparison, the flanging degree of the tube in the system with the field shaper is greater, and the final deformation of the tube is shown in Fig. 12.

4.2 The energy consumption

In the electromagnetic flanging process, the energy storage capacitor discharges into the tube through the driving coil and makes it flanged under the action of electromagnetic force. The electrical energy of the system is finally converted into deformation energy required for

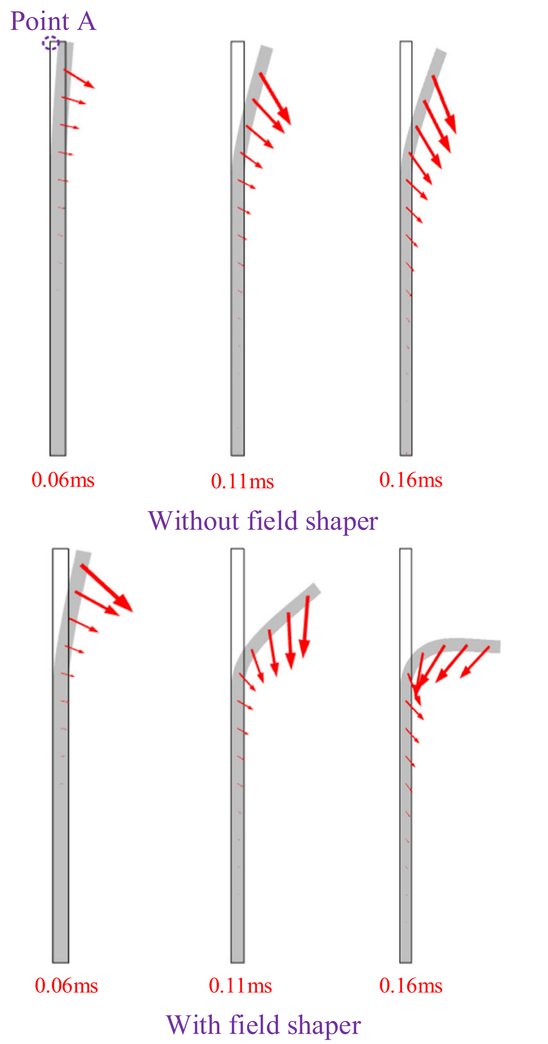

Fig. 10 Distribution of Lorentz force vector at the end of the tube

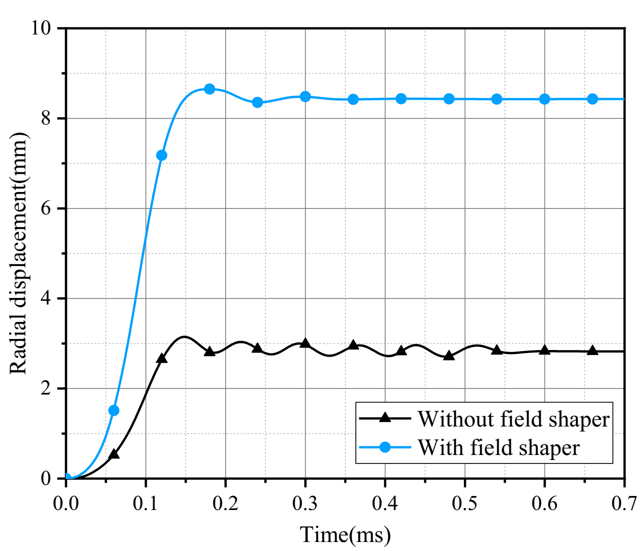

Fig. 11 Calculated radial displacements at point A

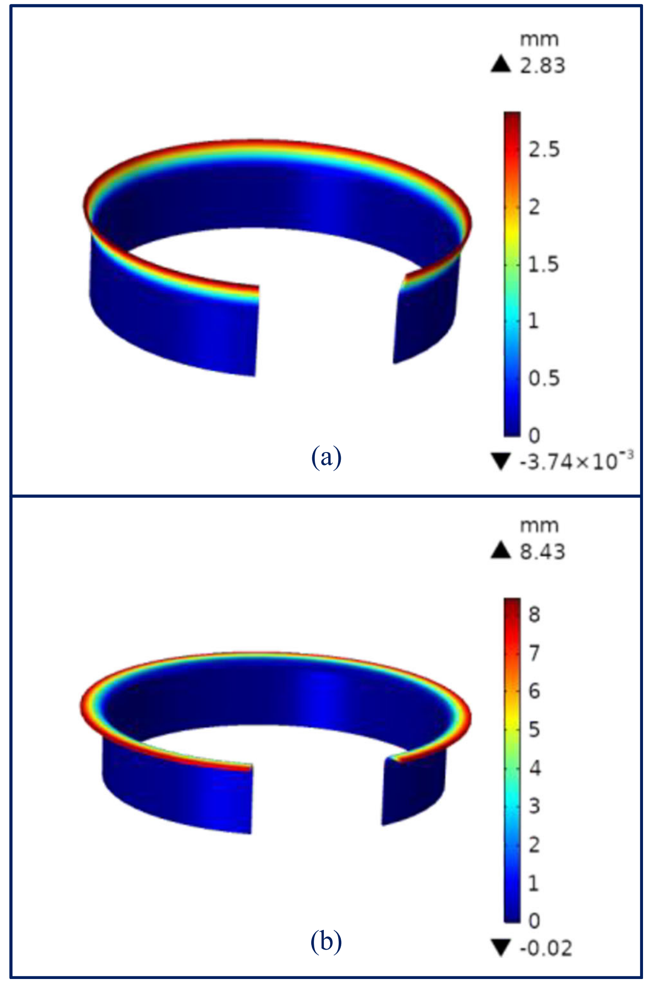

Fig. 12 3D simulation deformation diagram: (**a**) without field shaper; (**b**) with field shaper

tube flanging. The discharge energy is an important parameter in electromagnetic flanging, which is directly related to processing calculation and the quality of the tube. Figures 8c and 13 show the flanging effect of tubes with the same inner diameter (110mm). By comparing the two models, it can be concluded that the degree of tube flanging is the same (θ_3=θ_4=90°). When other conditions are the same, the discharge voltage of the system with and without the field shaper is 4.6kV and 5.3kV, respectively. The discharge energy of the system can be expressed as:

$$W = \frac{1}{2} C U^2 \tag{13}$$

where W is the discharge energy and C and $\boldsymbol{U}$ are the capacitor capacitance and the discharge voltage. According to the above equation, the discharge energy of the system with and without the field shaper can be calculated as 1.69kJ and 2.25kJ, respectively. Obviously, it can be found that adding a field shaper can save 25%

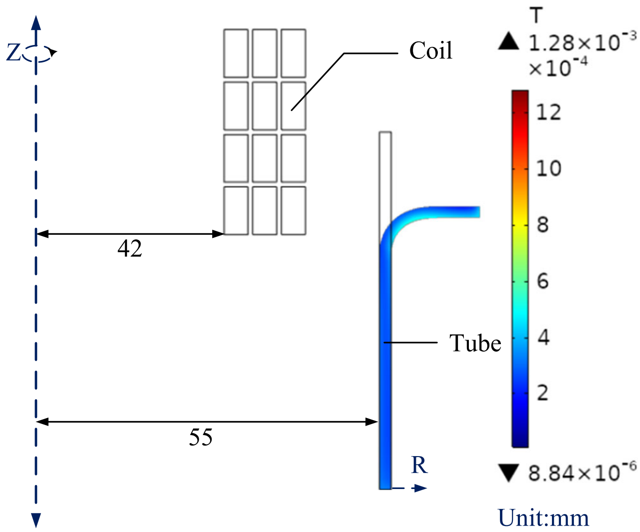

Fig. 13 Schematic diagram of 110mm tube flanging without field shaper

of the energy consumption for the entire electromagnetic flanging system.

4.3 The flexibility

Since the electromagnetic force decays rapidly with the increase of distance, different coils need to be wound when forming different tubes. The inner diameter of the tubes is increased to 120mm as shown in Fig. 14. It can be found that in the system without a field shaper, the tube is difficult to achieve the previous effect due to the limitation of distance. Therefore, a larger coil needs to be replaced in the system. With the same discharge energy (2.09kJ), the inner diameter of the forming coil is increased from the original 84 to 94.8mm as shown in Fig. 14a. At this time, the thickness of the field shaper is 9mm. It can be seen that the tube has achieved the ideal flanging effect (θ_5=90°). Although the flanging of different tubes can be realized by changing the coil, it will raise the cost of the whole system and the complexity of the process. The manufacturing process of the forming coil is as follows: First, the corresponding size of the coil bobbin needs to be processed according to the designed scheme, and then the corresponding copper wire is selected for winding on the winding machine. After the coil is wound, it is reinforced with glass fiber and then reinforced with epoxy resin. At the same time, a special "copper nose" must be made, whose function is to connect the incoming and outgoing wires of the coil with the external circuit. It can be seen that the manufacturing process of the forming coil is very complicated. In addition, the raw materials such as reinforcing fiber and epoxy resin used in the winding process are very expensive, and the cost caused by frequent replacement of coils is also very high.

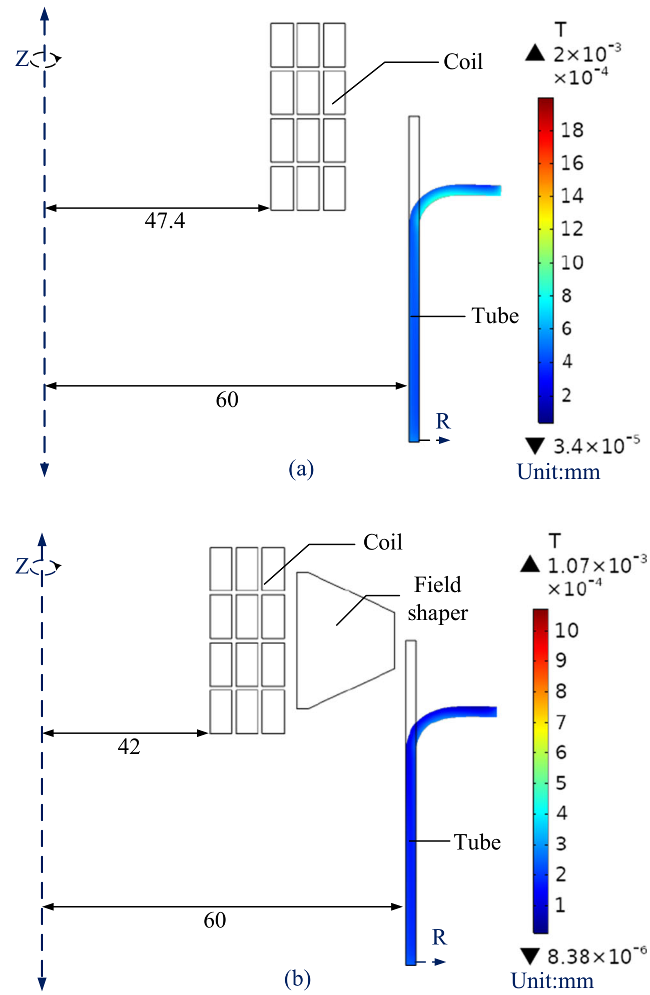

Fig. 14 Schematic diagram of 120mm tube flanging: (**a**) without field shaper; (**b**) with field shaper

Consequently, a filed shaper can be introduced into the existing electromagnetic flanging device without replacing the coil, as shown in Fig. 14b. Workers only need to cut the copper block into the required shape on the machine tool to complete the processing of the field shaper, which is very simple. In this article, the field shaper is made of the same material as the forming coil. The materials needed to make the field shaper are also cheaper than those for the forming coil. Hence, the method of adding the field shaper brings great flexibility and cost reduction to the existing electromagnetic flanging system.

5 Conclusions

To overcome the shortcomings of the traditional electromagnetic flanging process, a field shaper is introduced to optimize the process. Our results show that (1) the flanging angle of the tube (defined as θ) can be increased from 13° in model 1 and

0° in model 2 to 90° in model 3 where a field shaper is introduced into the system. (2) When forming a tube with an inner diameter of 110mm, the discharge voltage can be tuned down from 5.3kV, without the field shaper, to 4.6kV, with the field shaper. That means the energy consumption of the system can be saved by 25%. (3) The manufacturing process of the field shaper is simpler than that of the forming coil, and the cost of the field shaper is lower. In summary, the introduction of a field shaper brings great flexibility to the tube flanging process and improves the economy of the system.

Acknowledgements The authors would like to thank Xiang Zhao, Xiangyi Liu, and Khan Christear Ahmed for their contributions in the writing process and also want to thank the support by the funding.

Author contribution Qi Xiong: Conceptualization, methodology, formal analysis, writing. Zhe Li: Methodology, software, investigation, writing-original draft preparation. Jianhua Tang: Formal analysis. Hang Zhou: Software, visualization. Meng Yang: Software, methodology. Xianqi Song: Investigation.

Funding This work was supported by the National Natural Science Foundation of China (NSFC) under Project Numbers 51707104, the State Scholarship Fund of China under Project Numbers 201908420196, and Sponsored by Research Fund for Excellent Dissertation of China Three Gorges University under Project Numbers 2021SSPY072.

Data availability All the data have been presented in the manuscript.

Code availability Not applicable.

Declarations

Conflict of interest The authors declare no competing interests.

References

1. Psyk V, Risch D, Kinsey BL, Tekkaya AE, Kleiner M (2011) Electromagnetic forming—a review. J Mater Process Technol 211(5):787–829
2. Belloir F, Huez R, Billat A (2000) A smart flat-coil eddy-current sensor for metal-tag recognition. Meas Sci Technol 11(4):367–374
3. Yu H, Jiang H, Li C (2012) Investigations on flanging of aluminum alloy tube under pulsed magnetic force. Iron Steel Res Int 19:438–441
4. Xiong Q, Huang H, Xia L, Tang H, Qiu L (2019) A research based on advance dual-coil electromagnetic forming method on flanging of small-size tubes. Int J Adv Manuf Technol 102(9-12):4087–4094
5. Gharghabi P, Dordizadeh P, Niayesh K (2011) Impact of metal thickness and field shaper on the time-varying processes during impulse electromagnetic forming in tubular geometries. J Korean Phys Soc 59(61):3560–3566
6. Rajak AK, Kumar R, Basumatary H, Kore SD (2018) Numerical and experimental study on effect of different types of field-shaper on electromagnetic terminal-wire crimping process. Int J Precis Eng Manuf 19(3):453–459
7. Zhang H, Liu N, Li X, Deng F, Wang Q, Ding H (2020) A novel field shaper with slow-varying central hole for electromagnetic pulse welding of sheet metal. Int J Adv Manuf Technol 108(7-8):2595–2606
8. Xiong Q, Yang M, Tang H, Huang H, Song X, Qiu L, Yu K, Cao Q (2020) Flaring forming of small tube based on electromagnetic attraction. IEEE Access 8:104753–104761
9. Karimi-nemch H, Sedighi M, Khandaei M (2016) Analysis of electromagnetic sheet metal forming process: experimental and FE study of mutual inductance and current pulse. Int J Appl Electrom 49(2):195–205
10. Cao Q, Lai Z, Xiong Q, Chen Q, Ding T, Han X, Li L (2016) Electromagnetic attractive forming of sheet metals by means of a dual-frequency discharge current: design and implementation. Int J Adv Manuf Technol 90(1-4):1–8.9
11. Qiu L, Deng K, Abu-Siada A, Xiong Q, Yi N, Fan Y, Tian J, Jiang J (2020) Construction and analysis of two-dimensional axisymmetric model of electromagnetic tube bulging with field shaper. IEEE Access 8:113713–113719
12. Xiong Q, Huang H, Deng C, Li L, Qiu L, Tang H (2018) A method to improve forming accuracy in electromagnetic forming of sheet metal. Int J Appl Electrom 57(3):367–375
13. Qiu L, Zhang W, Abu-Siada A, Xiong Q, Wang C, Xiao Y, Wang B, Li Y, Jiang J, Cao Q (2020) Electromagnetic force distribution and wall thickness reduction of three-coil electromagnetic tube bulging with axial compression. IEEE Access 8:21665–21675
14. Xiong Q, Yang M, Liu X, Song X, Qiu L, Jiang J, Yu K (2020) A dual-coil method for electromagnetic attraction forming of sheet metals. IEEE Access 8:92708–92717
15. Ouyang S, Li X, Li C, Du L, Peng T, Han X, Li L, Lai Z, Cao Q (2020) Investigation of the electromagnetic attractive forming utilizing a dual-coil system for tube bulging. J Manuf Process 49:102–115